Chemical Engineering Journal 151 (2009) 295–301

Contents lists available at ScienceDirect

Chemical Engineering Journal

journal homepage: www.elsevier.com/locate/cej

Photocatalytic decomposition of direct red 16 and kinetics analysis in a conic body packed bed reactor with nanostructure titania coated Raschig rings

J. Saien[a,*], M. Asgari[a], A.R. Soleymani[a], N. Taghavinia[b]

[a] Department of Applied Chemistry, Bu-Ali Sina University, Hamedan, 65174, Iran
[b] Institute for Nanoscience and Nanotechnology, Sharif University of Technology, Tehran 14588, Iran

ARTICLE INFO

Article history:
Received 5 October 2008
Received in revised form 25 February 2009
Accepted 3 March 2009

Keywords:
Photocatalytic degradation
Nanostructure TiO_2
Packed bed
Direct red 16
Kinetics

ABSTRACT

A conic body packed bed reactor, internally irradiated with a UV-C lamp and equipped with circulating upflow stream was employed to investigate the decomposition of a widely used azo dye, direct red 16, in water. The synthesized nanostructure TiO_2 photocatalyst particles were immobilized on the surface of transparent Raschig ring packings. Solutions with initial concentration of 30 mg L^{-1} of dye, within the range of typical concentration in textile waste waters, were treated under the mild operating conditions of natural pH of 6.75 and temperature of 25 °C. Investigations on the active species showed that hydroxyl radicals play the major role in the process, providing a perfect degradation in 90 min of irradiation and hence 93% in about 60 min; and also about 71% desired decomposition of aromatic groups in 120 min. For kinetic investigations, the rate of degradation of the dye was expressed as the sum of the rates of individual photolysis and photocatalysis process branches in power law model. Meanwhile, the Langmuir–Hinshelwood kinetic model describes the variations in pure photocatalytic branch in consistent with a first order power law model.

1. Introduction

Photocatalysis and other advanced oxidation processes (AOPs) play an important role in dealing with today's challenging demand for drinking water and waste water treatment technologies. A wide literature on this subject proves that photocatalytic oxidation reactions have the potential to completely mineralize organic compounds to carbon dioxide and to lead us to a 'clean and green purification technology' for treatment of polluted water and air [1,2].

Several semiconductors such as TiO_2, Fe_2O_3, ZnO, ZnS, CdS, WO_3 are known to have photocatalytic properties [3,4]. Among them, TiO_2 is the most widely used for its high photocatalytic activity, stability, non-toxicity and low price [2,5]. A wide literature on this subject proves that the UV-irradiated titania surface can generate highly oxidative electrical holes to decompose various organic compounds present in aqueous and gaseous streams at ambient temperature and pressure conditions [6].

A problem, encountering in photocatalytic degradation, is conventional powder catalysts, used in usual slurry photocatalytic reactors, suffer from disadvantages in stirring during the reaction, in separation after the reaction and in fast fouling of the UV lamp; especially when the valuable nanoparticles are used. These problems present a major drawback for the commercial application of slurry photocatalytic reactors for treating waste water. Alternatively, the catalyst may be immobilized onto a solid inert support and used as immobilized film which eliminates the need of removing the catalyst from water. Unfortunately, when the catalyst is immobilized, there will be a decrease in the available surface area for the reaction since the catalyst must adhere to the solid support unless the substrate was UV transparent, thus the reactor design is limited by the optical absorption constraints.

In the last 10 years several works have been developed for the deposition of photoactive materials on inert bodies to be used in fixed-bed reactors. The emphasis has been to determine the reaction kinetics equations. A number of substrates that photocatalyst is immobilized on their surfaces are glass spheres, pyrex and polystyrene beads, fiber glass, quartz optical fibers, ceramic membranes and monoliths, stainless steel (flat and corrugated plates), zeolites and anodized iron [7–13].

Different alternatives are still remained to be investigated in this area; including the place and the power of the UV lamp for a proper configuration, and improving the activity for the whole reactor with efficient fluid hydrodynamic.

The main purpose of the present study is to develop a novel photocatalytic reactor with immobilized home prepared TiO_2 nanoparticles on the transparent quartz packings, exposed to direct and internal UV irradiation for purification of water from an azo dye, C.I. direct red 16 (C.I. 27680) (DR16) with no previous report about its photo-degradation, finding the optimum conditions to achieve the maximum degradation and obtaining the details.

* Corresponding author. Tel.: +98 811 8282807; fax: +98 811 8257407.
E-mail address: saien@basu.ac.ir (J. Saien).

1385-8947/$ – see front matter © 2009 Elsevier B.V. All rights reserved.
doi:10.1016/j.cej.2009.03.011

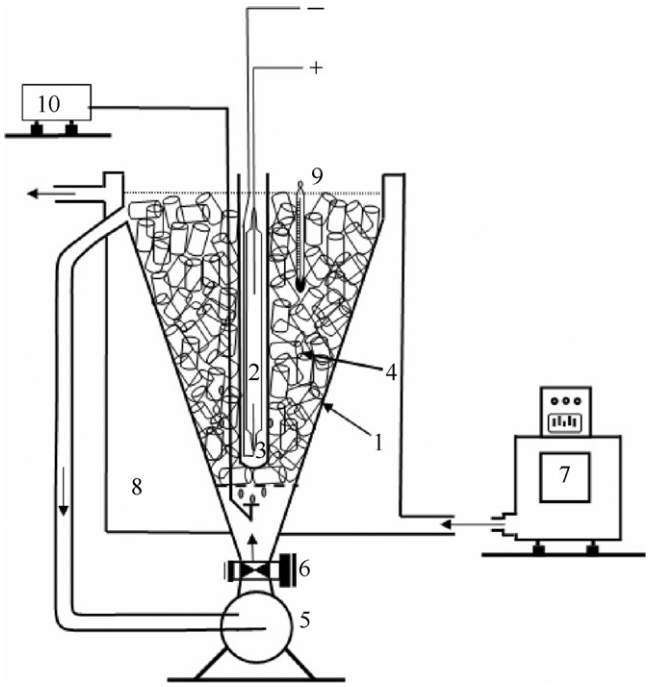

Fig. 1. Sketch of the experimental apparatus: (1) reactor body; (2) UV lamp; (3) quartz tube; (4) TiO_2 coated Raschig rings; (5) circulating pump; (6) valve; (7) thermostat; (8) cooling jacket; (9) thermometer; (10) micro-air compressor.

2. Experimental

2.1. The reactor

As a result of well known requirements for an efficient photoreactor, including a large irradiated catalyst surface area and enough receiving of emitted photons, as well as satisfactory mass transfer capacity [14]; a novel device was used in this study (Fig. 1). A packed bed annular and symmetric vertical reactor with a conic body shape and capacity of about 1 L benefits an immersed symmetrically UV lamp (mercury 150 W, UV-C, medium pressure, manufactured by ARDA, French). The lamp was surrounded with randomly filled packings of titania coated quartz Raschig rings, each with the size of 15 mm height, 7.25 mm out diameter and thickness of 1 mm. Note that these sizes were chosen based on the allowable pressure drop for pilot and full-scale testing of this technology. This arrangement makes possible the light absorption of the catalytic layer in the whole space of packed bed.

A pump, located below the reactor, provides an adjustable upflow circulating stream. Since the photocatalysis is sustained by a ready supply of dissolved oxygen, air was bubbled through the reactor at a constant flow rate using a small air compressor to ensure sufficient oxygen exposure. The air flow and the circulating stream helps the well mixing of the reactor content in order to overcome mass transfer resistance and inhibit formation of dead zones in the reactor. The reactor was equipped with a water-flow jacket for regulating the temperature by means of an external circulating flow of a thermostat bath (OPTIMA-740, Japan) with an accuracy of ±0.1 °C. The whole reactor body was covered with an aluminum thin layer to prevent UV emission around it.

2.2. Reagents

All reagents were used as received without further purification. The azo dye, direct red 16, $C_{26}H_{17}N_5Na_2O_8S_2$ (C.I. 27680, MW 637.26) was purchased from Alvan Sabet company, 99% pure. Fig. 2 displays the structure of this dye. Sulfuric acid and sodium hydroxide, used to adjust the pH of solutions and ethanol, used to quench the hydroxyl radicals, were all Merck products.

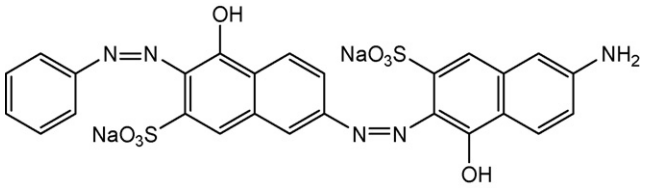

Fig. 2. The chemical structure of C.I. direct red 16 (DR16).

2.3. Procedures

2.3.1. Catalyst synthesis and coating

Colloidal suspension of TiO_2 nanostructure particles was synthesized by mixing titanumtetraisopropoxide (TTIP), H_2O_2 and H_2O, with volume proportions of 12:90:200, respectively. The resulting solution was refluxed for 10 h to promote the crystal structure. The ion conductivity of the synthesized TiO_2 sol was 200 μS/cm. Zeta potential of the particles was measured to be −50 mV which is sufficiently large to keep the suspension stable. TiO_2 particles were totally in the form of anatase and BET surface area of about 84 m^2/g.

To immobilization of the catalyst, 20 cm pieces of quartz tubes were first washed with acid and double distilled water and then coated by dip coating in the mentioned colloidal suspension. The immersing and withdrawal speed was 9 mm/s. The tubes were deposited for three times, each time withdrawn from the opposite end. After drying in isolated ambient temperature, the tubes were heated at 200 °C for 10 min. Finally calcination was done for 1 h in an oven at 500 °C to well attaching the TiO_2 nanoparticles on the tube surface. After being washed with deionized water, the tubes were dried at about 100 °C. In this way a transparent, high purity thin film was deposited. The coated quartz tubes were finally divided into Raschig ring pieces, each with the length of 15 mm. Recently, a similar method for coating TiO_2 thin film on a glass substrate has been reported. An aqueous solution of TiO_2-HF with the addition of boric acid as a free F^- scavenger has been used [15].

2.3.2. Performance of experiments

Before each experimental run, the reactor system was cleaned by circulating distilled water through it for about 5 min without illumination. This procedure allowed the removal of any residual compounds from previous runs. In order to perform the runs, solutions containing initial concentration of 30 mg L^{-1} of dye (about 5×10^{-5} M) which is within the range of typical concentration in textile waste-waters [16] were prepared. The pH was adjusted to the desired value by means of a pH meter (Denver, UB-10) using dilute H_2SO_4 or NaOH solutions. After transferring the solution into the reactor, the lamp was switched on to initiate the irradiation, while the temperature was adjusted. Samples (4 mL) were taken at regular times to analyze the content. A maximum total sampling volume of 36 mL was withdrawn during each series of experiments. This volume is not significant compared with the reactor capacity.

2.3.3. Analysis methods

The concentration of the dye in each sample was analyzed with a UV–vis spectrophotometer (PerkinElmer, 55 OSE), measuring the absorbance at λ_{max} = 526.6 nm and using the appropriate calibration curve (Fig. 3). It is notable that the maximum wavelength and the molar absorption coefficient of DR16 were not much dependent on the pH of solution within the range of 4–10. Using this method, the degradation efficiency (X) of DR16 with respect to its initial

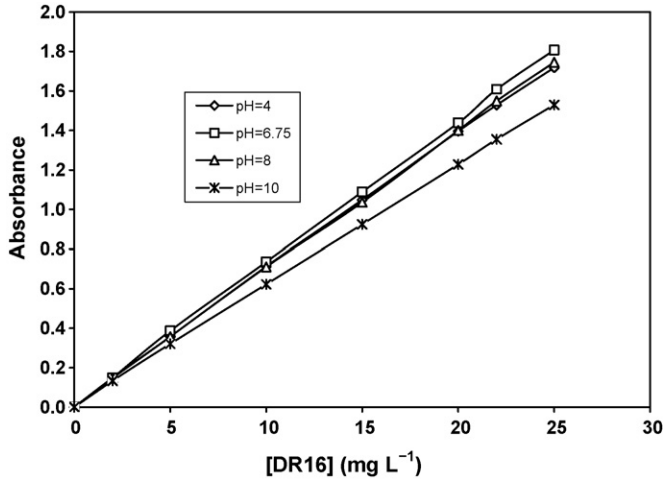

Fig. 3. The calibration curves for measuring DR16 concentration at different pH values and 25 °C.

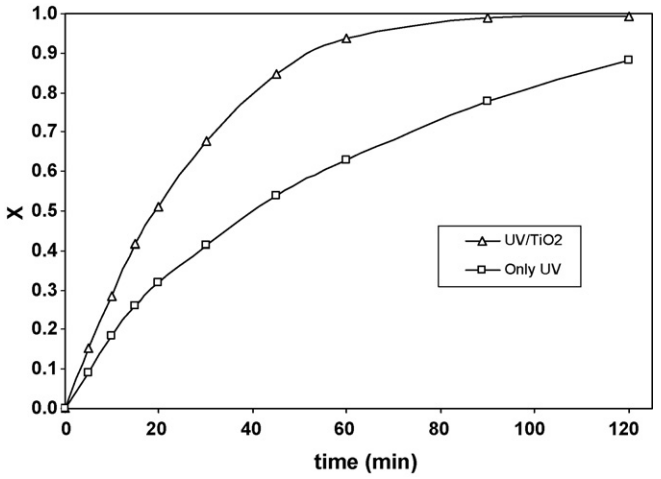

Fig. 5. The role of coated nano TiO_2 particles on degradation of DR16; natural pH and 25 °C.

concentration was calculated as follows:

$$X = \frac{[DR16]_o - [DR16]}{[DR16]_o} \quad (1)$$

where $[DR16]_o$ and [DR16] are the initial and appropriate time concentrations of DR16.

In order to follow the decomposition of the aromatic groups, high-performance liquid chromatograms at different times were recorded by a HPLC (PerkinElmer Series 200). An Agilent Zorbax 80 Å Extend C18 column with dimension of 2.1 mm × 100 mm, particle size of 3.5 μm and a UV–vis detector with the wavelength set at 254 nm were used. The mobile phase was a mixture of methanol-ammonium acetate (3.8 g L^{-1}), 30/70 (v/v) at a flow rate of 0.2 mL min^{-1}.

3. Results and discussion

3.1. UV–vis spectra

In a precedent study, the UV–vis absorption spectra of DR16 were studied at different times of irradiation under natural pH of 6.75 and 25 °C. As it is presented in Fig. 4, the bands relating to different molecular parts in this dye are decreased with respect to time. DR16 is a two azo dye in which the chromophore part of molecular structure contains azo linkage and shows a strong absorbance at 526.6 nm in the visible region [17]. The absorbance peak at 526.6 nm is attributed to azo linkage. The decrease of peaks at this wavelength indicates a rapid degradation of azo dye from the–N=N double bond as the most active site for the oxidation attack [18]. The nearly perfect disappearance of the band at 526.6 nm reveals that DR16 is eliminated after about 90 min. In our previous work a 93% degradation of azo dye direct blue 71 has been reported in a similar reactor with slurry fluid and freely suspended TiO_2 particles, after about 120 min [19].

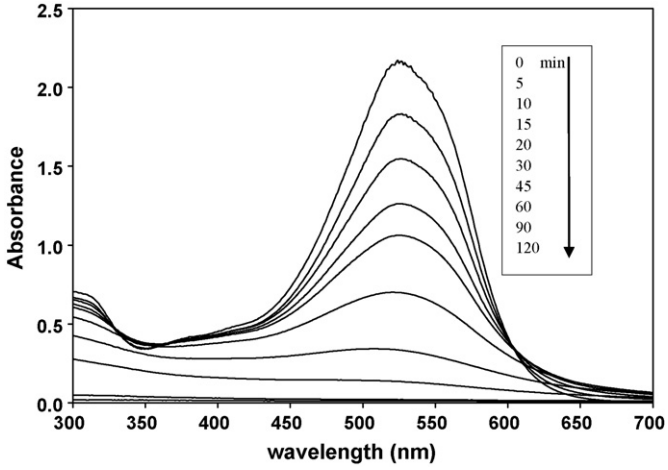

Fig. 4. UV–vis spectra changes of DR16 at different times during photocatalysis process; natural pH and 25 °C.

3.2. Investigations on the degradation reaction

In order to investigate the role of photocatalysts, experiments were performed for the only photolysis degradation while the reactor was filled with inert quartz packings. Fig. 5 compares the variations of photolysis and photocatalysis degradation of DR16. A nearly perfect degradation is achieved in an irradiation time of 90 min; under its natural pH (6.75) and 25 °C; however, the efficiency reaches to only about 78% at the same conditions in photolysis. It is obvious that a part of degradation will be conducted in photolysis branch while the photocatalysis degradation is in progress. Fig. 5 also shows that the degradation trend is significantly high for the photocatalysis process till about 60 min, for which a degradation efficiency of about 93% is achieved.

The more activity of the UV/TiO_2 process is due to the well-known electron promotion from the valance band to the conduction band of the semi-conducting oxide to give electron–hole pairs [20,21]. The valance band hole (h^+_{VB}) potential is positive enough to generate hydroxyl radicals at the surface. Moreover, the conduction band electron (e^-_{CB}) is negative enough to reduce the oxygen molecules, present in the solution. The generated hydroxyl radicals are powerful oxidizing agents and attack organic pollutants, present at the surface of TiO_2 or near it (within 500 nm) and of course the reaction rate of hydroxyl radicals with pollutants decreases as the distance from the catalyst surface increases [22]. It is remarkable that there was no change in dye concentration, when the reactor was used in darkness; i.e. no decrease in dye concentration can be attributed due to the physical adsorption of the dye on the surface.

3.3. Effect of pH

Fig. 6 demonstrates the effect of pH within the range of 4–10. The degradation efficiency finds the highest values with the pH values

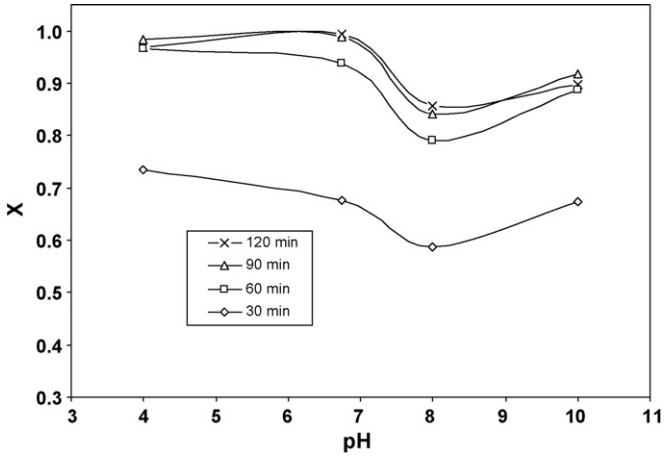

Fig. 6. Effect of pH on photocatalytic degradation of DR16 after different irradiation times; 25 °C.

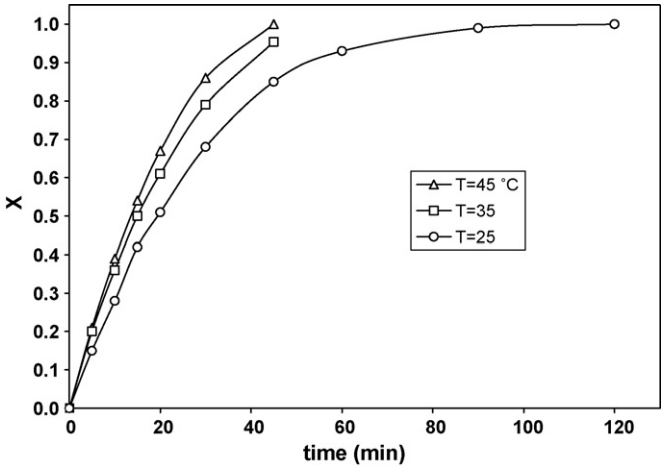

Fig. 7. Effect of temperature on photocatalytic degradation of DR16; natural pH.

within 4–6.75. The reason is that according to the pH of zero point of charge of TiO_2 which is 6.25 or 6.8 [23,24], its surface is presumably positively charged and since the dye has negative charge sulfite groups, the acidic solution favors the adsorption of dye onto the catalyst surface or at least causing to find closer position to it. An enhancement in degradation via direct oxidation or reduction by active species is therefore will be provided. The formation of OH radicals in acidic solution can be another reason, as it can be inferred from the following reactions [25]:

$$e^-_{CB} + O_2(ads) \rightarrow O_2^{\bullet -} \quad (2)$$

$$O_2^{\bullet -} + H^+ \rightarrow HO_2^{\bullet} \quad (3)$$

$$2HO_2^{\bullet} \rightarrow O_2 + H_2O_2 \quad (4)$$

$$H_2O_2 + O_2^{\bullet -} \rightarrow {}^{\bullet}OH + OH^- + O_2 \quad (5)$$

The decrease in degradation efficiency within pH values 7–8 could be commented by existence of some repulsion between the negatively catalyst surface charged and negative charge sulfite and hydroxyl ions. This will suppress the degradation via active species on the catalyst surface. The degradation efficiency at pH value of 10 has found some enhancement. It could be due to the more abundant of hydroxyl ions that more easily generate hydroxyl radicals, thus the efficiency of the process is logically increased [26].

The natural pH of 6.75 can be chosen as a moderate and optimum pH value and the experiments were followed under this pH, having the advantage of no need to add agents in order to regulate the pH of solution.

3.4. Effect of temperature

In the range of 25–45 °C, an enhancement (about 17% after 45 min) in the dye degradation efficiency was observed (Fig. 7). This rather low practical influence must be due to the low activation energy of photocatalytic reactions, for example 5.5 kJ mol^{-1} [27] and 8.24 kJ mol^{-1} [28]; however, an increase in temperature helps the degradation reaction to compete more effectively with $e^-_{CB} - h^+_{VB}$ recombination. On the other hand, the increase in temperature decreases the solubility of oxygen in water which is not desirable. The maximum temperature of 45 °C can be adapted at which a degradation efficiency of about 100% of dye is achieved in 45 min. Higher temperatures will cause evaporation of the solutions during the experiments.

3.5. Investigation on active species

It is well known that in the photocatalytic degradation process two main species have the major contributions: (1) electrons and holes (h^+_{VB}, e^-_{CB}), (2) hydroxyl radicals. The importance of these depends on the substrate structure and operational parameters such as pH. The activity of these species can be distinguished using a radical scavenger [19,29]. Alcohols such as ethanol are commonly used to quench hydroxyl radicals because of completely high rate constant of reaction between hydroxyl radicals and ethanol (19×10^9 M^{-1} s^{-1}) [29]. In this regard, photolysis (with inert quartz packings) and photocatalysis experiments were performed, each of them with different amounts of added ethanol under natural pH and 25 °C. Figs. 8 and 9 present these results respectively. Adding ethanol till 0.06 volumetric percentages (v/v) has led to a decrease in degradation efficiency for the both processes. The observed reduction by adding ethanol up to 0.06% is due to the quench of hydroxyl radicals by the ethanol molecules and therefore can be introduced as the role of hydroxyl radicals in the process. Adding extra amounts of ethanol causes the degradation efficiency to increase. The formation of ethoxy radicals ($C_2H_5O^{\bullet}$) from direct photocatalytic oxidation of ethanol can help in this regard. The ethanol molecules on the other hand, can produce hydroxyl radicals in direct photolysis with respect to the level of C–O energy bond [30].

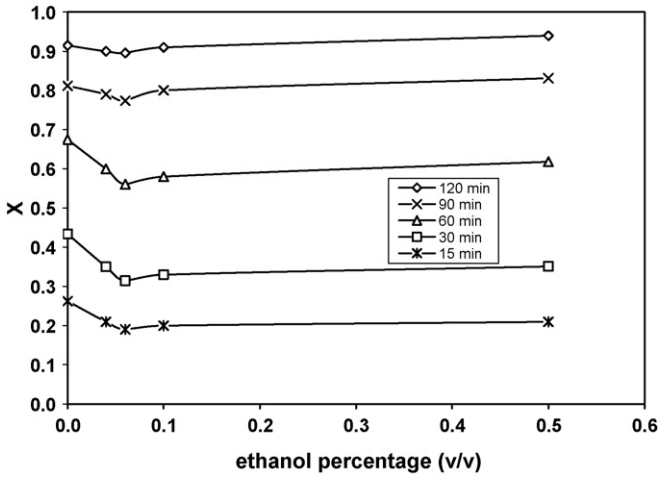

Fig. 8. Variation of the degradation of DR16 in photolysis process versus added amounts of ethanol at different irradiation times; natural pH and 25 °C.

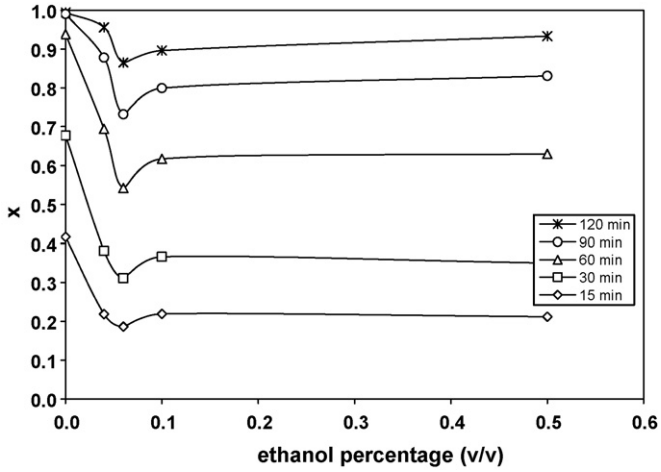

Fig. 9. Variation of the degradation of DR16 in photocatalysis process versus added amounts of ethanol at different irradiation times; natural pH and 25 °C.

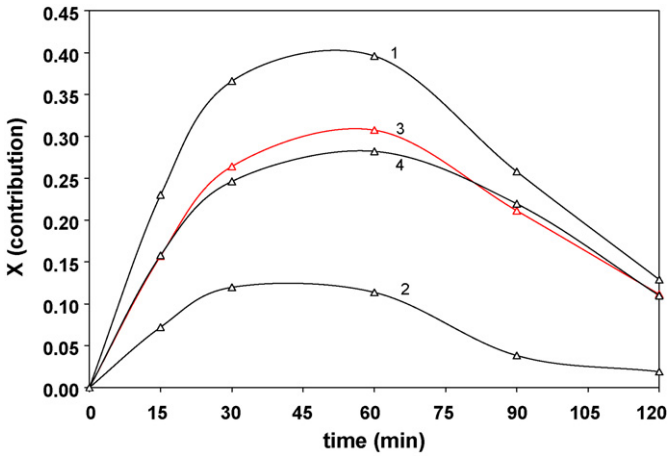

Fig. 10. The contribution of active species in degradation efficiency; (1) OH radicals in photocatalysis process, (2) OH radicals in photolysis process, (3) OH radicals generated by catalyst (difference between curves 1 and 2) and (4) presence of catalyst totally; natural pH and 25 °C.

We benefit from the above results and those from Section 3.2 for investigating on contribution of different active species in the reaction progress.

The variation in the amounts of degradation efficiencies, between the cases of no added ethanol and with 0.06% of ethanol, in fact represents the variation of contribution of hydroxyl radicals in the photolysis and photocatalysis processes (curves 1 and 2 in Fig. 10). Also, the difference between these two items represents the contribution of hydroxyl radicals appropriate to the presence of catalyst (curve 3 in Fig. 10). On the other hand, the difference between the two items indicated in Fig. 5 can be considered as the total contribution of the catalyst in the degradation process (curve 4 in Fig. 10).

From Fig. 10 two kinds of conclusion can be deduced: (i) the closeness of curves 3 and 4 reveals that the hydroxyl radicals is the most important active species in degradation of the dye by the catalyst, and degradation directly via h^{+}_{VB} and e^{-}_{CB} is negligible, and (ii) the highest level of catalyst contribution in dye degradation takes place within the time range of 30–60 min. The reason can be due to

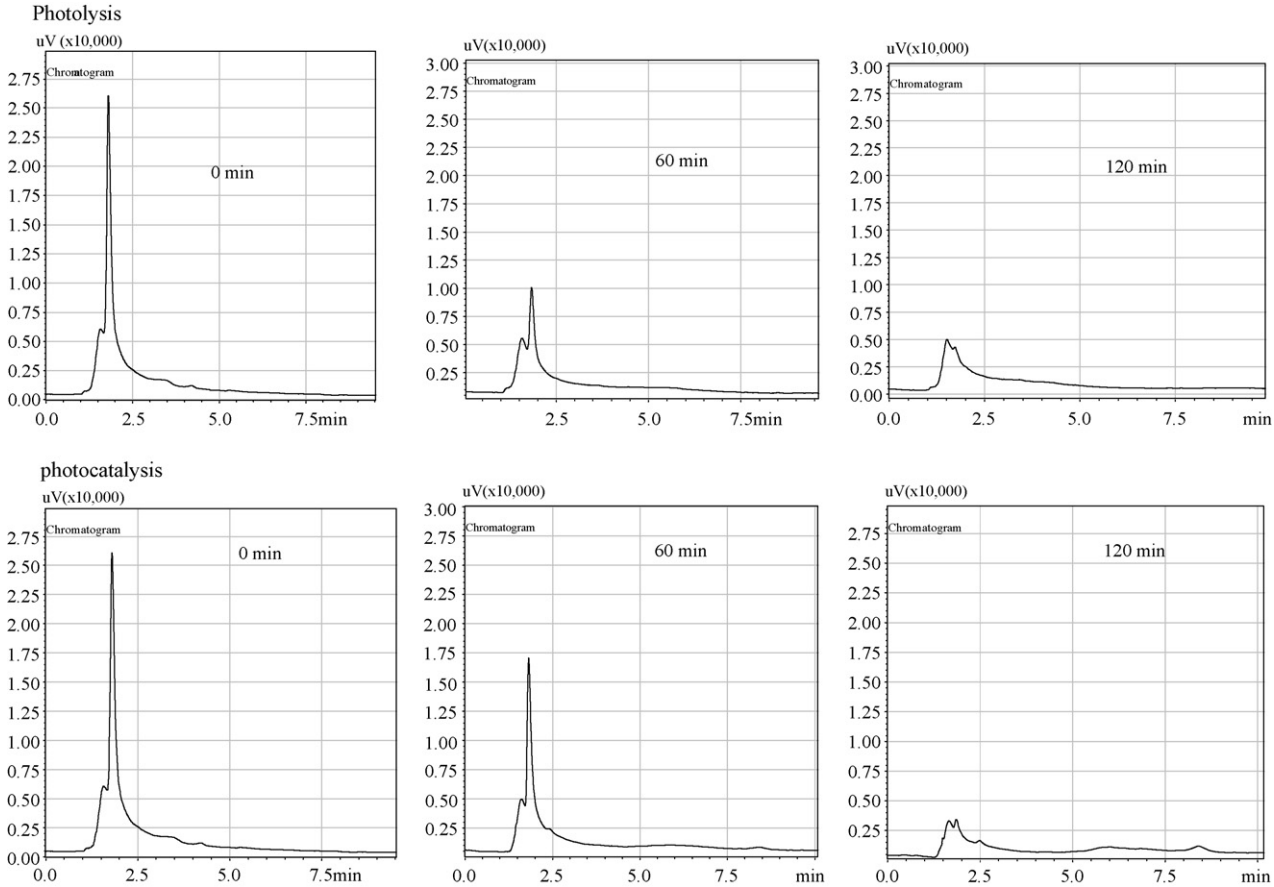

Fig. 11. The HPLC chromatograms of samples at different times of degradation; natural pH and 25 °C.

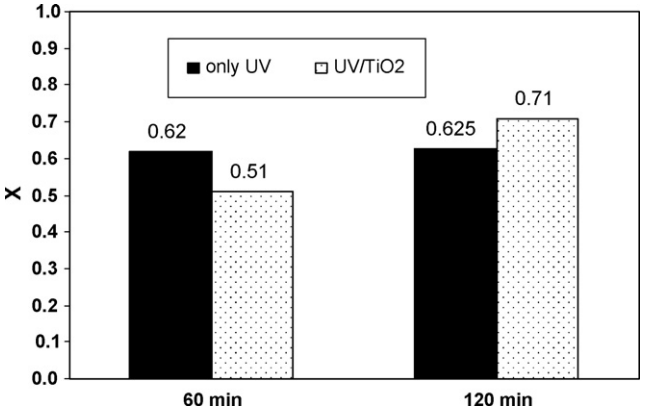

Fig. 12. The conversion of aromatic content for photolysis and photocatlysis processes after 60 and 120 min of irradiations; natural pH and 25 °C.

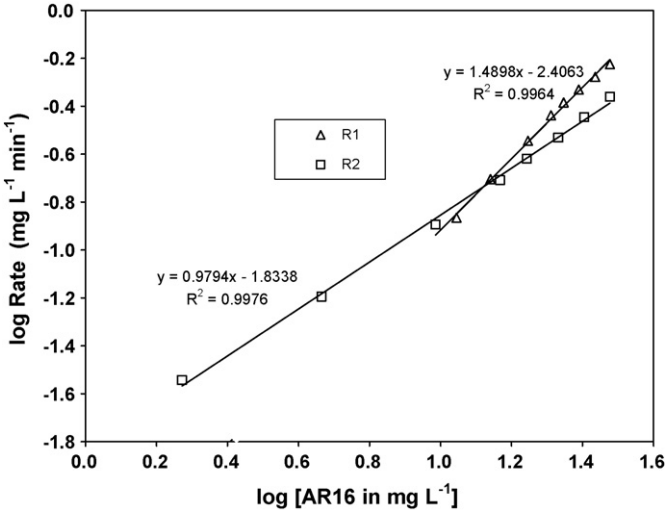

Fig. 13. Variation of the rate of degradation of DR16 versus its concentration for photolysis and photocatalysis branches; natural pH and 25 °C.

the formation of stable intermediate molecules after about 60 min of degradation and therefore engaging a part of catalyst activity on interaction with intermediates.

3.6. HPLC analysis

The HPLC chromatograms of the samples, taken for the both cases of photolysis and photocatalysis at the beginning, after 60 and 120 min of irradiation are presented in Fig. 11. The absorbance peaks of the benzene and naphthalene rings are appeared in the UV region (254 nm) [31]. It is obvious that the amount of aromatic groups decreases as the decreasing of peaks. At the beginning of the process, a peak appropriate to DR16 molecule is observed (retention time of 2 min) which diminishes with progress in the process. No other peak, relating to intermediates, is observed in the chromatograms, perhaps due to the same polarity of the aromatic intermediates with DR16 molecules.

The peak area is a criterion of the remaining aromatic rings in the solution. The appropriate conversion (or efficiency) based on the peak areas are presented in Fig. 12. The figure shows that after 60 min of irradiation, the aromatic content for the photolysis is less than that of the photocatalysis (62% conversion compared with 51%). The reason is due to the more abundance of aromatic intermediates, generated by the non-selective attack of active species to the dye molecules in the photocatalysis process. By the end of the processes (after 120 min) the conversion parameter for the photocatalysis reaches to 71% while this parameter remains nearly constant for the photolysis process. This matter reflects the effectiveness of the active species, produced by the catalyst, in the vital case of aromatic decomposition.

3.7. Kinetic studies

Due to the practical applications, the degradation kinetics of DR16 was investigated under the preferred conditions of natural pH and 25 °C. As was explained in Section 3.2, the net degradation reaction is the result of two parallel activities of photolysis and photocatalysis (assuming negligible turbidity of very thin layer catalyst);

$$R = -\frac{\mathrm{d[DR16]}}{\mathrm{d}t} = R_1 + R_2 \tag{6}$$

where R, R_1 and R_2 are the net degradation, the individual pure photolysis and photocatalysis rates, respectively. The difference between the net potocatalysis and photolysis rates can be considered as the rate of pure photocatalytic reaction rate.

The differential method of analysis, based on the data of concentration versus time with at least eight data points was employed. Based on the provided data, the power law kinetic model showed a nice agreement with experimental data for both photolysis and photocatalysis branches of the process up to 60 min of degradation;

$$R = k_1[\mathrm{DR16}]^{n_1} + k_2[\mathrm{DR16}]^{n_2} \tag{7}$$

where n_1, n_2, k_1 and k_2 are the appropriate orders of reactions and the rate constants. Fig. 13 presents the goodness of fitting with Eq. (7) with the data. The obtained kinetic parameters, in addition to the coefficient of determination (R^2) for each case are given in Table 1. For decomposition of sodium dodecylbenzene sulfonate solution, for instance, an order of 1.32 [32], and for degradation of Auramine O [33] a second order, have been reported.

Using Langmuir–Hinshelwood (L–H) kinetic expression [14,34] which is based on the adsorption of substrate on the surface of catalyst, also gives nice agreement for the modeling of photocatalytic branch rates, up to 60 min. The modified L–H equation is given by:

$$R_2 = -\frac{\mathrm{d[DR16]}}{\mathrm{d}t} = \frac{k_r K[\mathrm{DR16}]}{1 + K[\mathrm{DR16}]} \tag{8}$$

where k_r and K are the reaction rate constant and the reactant adsorption constant respectively. By plotting the reciprocal of photocatalytic degradation rate ($1/R_2$) against the reciprocal of dye concentration, 1/[DR16], at different times (Fig. 14), a linear variation was observed and the values of k_r and K were found to be 1.66 mg L^{-1} min^{-1} and 9.27 × 10^{-3} L mg^{-1}, respectively (R^2 = 0.9997).

The photocatalytic degradation kinetic in power law expression is first order. On the other hand, a pseudo first order kinetic can be deduced from L–H model if a low substrate concentration can be attributed, i.e. at the beginning of the process where: $K[\mathrm{DR16}] \ll 1$.

Table 1
Kinetic parameters of DR16 degradation during 60 min.

n_1	k_1	R^2	n_2	k_2	R^2
1.49	3.98×10^{-3} (mg L^{-1})$^{-0.49}$ min^{-1}	0.996	0.98	1.47×10^{-2} (mg L^{-1})$^{0.02}$ min^{-1}	0.998

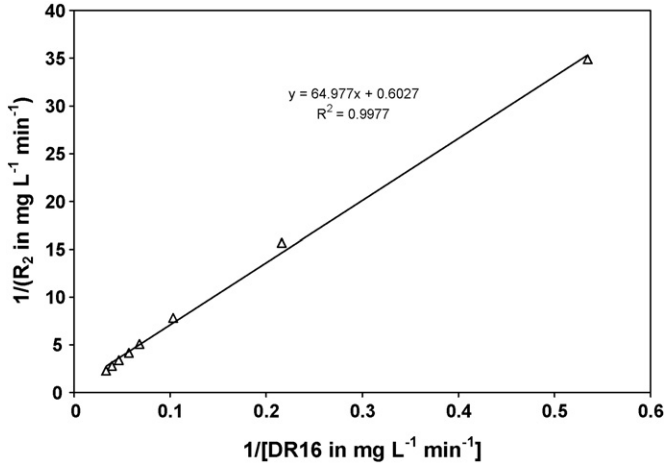

Fig. 14. Variation of inverse of DR16 degradation rate versus its inverse concentration for the photocatalysis branch; natural pH and 25 °C.

The above analysis confirms the points given in Section 3.5 and that the dominant degradation takes place at the surface of the catalyst via OH radicals.

4. Conclusions

A perfect degradation of direct red 16 in water is achievable using a developed packed bed photoreactor with coated nanostructure TiO_2 packings and internally irradiated under mild conditions after about 90 min. In shorter times of irradiation, the degradation efficiency can reach to 93% after about 60 min of irradiation. This time is appropriate for a high trend of degradation by the coated catalysts in the reactor.

The hydroxyl radicals at the surface of coated packings play as the most active species in the photocatalytic process. It was revealed that for the vital case of aromatic decomposition, the photocatalytic process provides a higher efficiency subject to irradiation times more than 60 min and hence it is vice versa in shorter irradiation times.

A satisfied procedure can be employed to determine the portion of degradation rate in photocatalysis and photolysis branches. The appropriate models of power law showed very nice goodness of fitting with experimental data. Also, studies showed that either a Langmuir–Hinshelwood kinetic expression or a first order type kinetic equation can be used to describe the rate variation for the pure photocatalytic branch in the used packed bed reactor and with the most contribution between 30–60 min of irradiation.

References

[1] D.F. Ollis, H. Al-Ekabi, Photocatalytic Purification and Treatment of Water and Air, Elsevier, Amsterdam, 1993.
[2] L. Zhang, T. Kanki, N. Sano, A. Toyoda, Photocatalytic degradation of organic compounds in aqueous solution by a TiO_2-coated rotating-drum reactor using solar light, Solar Energy 70 (2001) 331–337.
[3] X. Domenech, Photocatalysis for Aqueos Phase De-Contamination; is TiO_2 the Better Choice, Elsevier, Amsterdam, 1993.
[4] T. Hasegawa, P.D. Mayo, Surface photochemistry: on the mechanism of the semiconductor-mediated isomerization of 4-substituted cis-stilbenes, Langmuir 2 (1986) 362–368.
[5] A. Alexiadis, I. Mazzarino, Design guidelines for fixed-bed photocatalytic reactors, Chem. Eng. Proc. 44 (2005) 453–459.
[6] D.M. Blake, Bibliography of work on the photocatalytic removal of hazardous compounds from water and air, NREL Report No. DE-AC36-99-GO10337 for the US Department of Energy, 2001.
[7] V. Loddo, S. Yurdakal, G. Palmisano, G.E. Imoberdorf, H.A. Irazoqui, O.M. Alfano, V. Augugliaro, H. Berber, L. Palmiano, Selective photocatalytic oxidation of 4-methoxybenzyl alcohol to p-anisaldehyde in organic-free water in a continuous annular fixed bed reactor, Int. J. Chem. React. Eng. 5 (2007) 1–15.
[8] M.E. Fabiyi, R.I. Skelton, Photocatalytic mineralization of methylene blue using buoyant TiO_2-coated polystyrene beads, J. Photochem. Photobiol. A: Chem. 132 (2000) 121–128.
[9] N.J. Peill, M.R. Hoffmann, Mathematical model of a photocatalytic fiber-optic cable reactor for heterogeneous photocatalysis, Environ. Sci. Technol. 32 (1998) 398–404.
[10] A. Alexiadis, 2D radiation field in photocatalytic channels of square, rectangular, equilateral triangular and isosceles triangular sections, Chem. Eng. Sci. 61 (2006) 516–523.
[11] C.R. Esterkin, A.C. Negro, O.M. Alfano, A.E. Cassano, Radiation field inside a reactor of glass-fiber meshes coated with TiO_2, AIChE J. 48 (2002) 832–845.
[12] H. Shang, Z. Zhang, W.A. Anderson, Non-uniform radiation modeling of corrugated plate photocatalytic reactor, AIChE J. 51 (2005) 2024–2033.
[13] G.E. Imoberdorf, H.A. Irazoqui, A.E. Cassano, O.M. Alfano, Photocatalytic degradation of tetrachloroethylene in gas phase on TiO_2 films: a kinetic study, Ind. Eng. Chem. Res. 44 (2005) 6075–6085.
[14] Z. Zhang, W.A. Anderson, M. Moo-Young, Experimental analysis of a corrugated plate photocatalytic reactor, Chem. Eng. J. 99 (2004) 145–152.
[15] N.S. Begum, H.M.F. Ahmed, Synthesis of nanocrystalline TiO_2 thin films by liquid phase deposition technique and its application for photocatalytic degradation studies, Bull. Mater. Sci. 31 (2008) 43–48.
[16] N. Daneshvar, A. Aleboyeh, A.R. Khataee, The evaluation of electrical energy per order (E_{Eo}) for photooxidative decolorization of four textile dye solutions by the kinetic model, Chemosphere 59 (2005) 761–767.
[17] W. Feng, D. Nansheng, H. Helin, Degradation mechanism of azo dye C.I. reactive red 2 by iron powder reduction and photooxidation in aqueous solutions, Chemosphere 41 (2000) 1233–1238.
[18] Z. Sun, Y. Chen, Q. Ke, Y. Yang, J. Yuan, Photocatalytic degradation of a cationic azo dye by TiO_2/bentonite nanocomposite, J. Photochem. Photobiol. A: Chem. 149 (2002) 169–174.
[19] J. Saien, A.R. Soleymani, Degradation and mineralization of direct blue 71 in a circulating upflow reactor by UV/TiO_2 process and employing a new method in kinetic study, J. Hazard. Mater. 144 (2007) 506–512.
[20] R.I. Bickley, M.J. Slater, W.J. Wang, Engineering development of a photocatalytic reactor for waste water treatment, Proc. Saf. Environ. Protect. 83 (2005) 205–216.
[21] W.J. Masschelein, Ultraviolet Light in Water and Wastewater Sanitation, Edited for English by R.G. Rice, Lewis Publishers, Boca Raton, 2002.
[22] A. Fujishima, T.N. Rao, D.A. Tryk, Titanium dioxide photocatalysis, J. Photochem. Photobiol. C: Photochem. Rev. 1 (2000) 1–21.
[23] M.R. Hoffmann, S.T. Martin, W. Choi, D.W. Bahnemann, Environmental applications of semiconductor photocatalysis, Chem. Rev. 95 (1995) 69–96.
[24] I.K. Konstantinou, T.A. Albanis, TiO_2-assisted photocatalytic degradation of azo dyes in aqueous solution: kinetic and mechanistic investigations, Appl. Catal. B: Environ. 49 (2004) 1–14.
[25] Y. Chen, Z. Sun, Y. Yang, Q. Ke, Heterogeneous photocatalytic oxidation of polyvinyl alcohol in water, J. Photochem. Photobiol. A: Chem. 142 (2001) 85–91.
[26] M.S.T. Goncalves, A.M.F. Oliveira-Campos, E.M.M.S. Pinto, P.M.S. Plasencia, M.J.R.P. Queiroz, Photochemical treatment of solutions of azo dyes containing TiO_2, Chemosphere 39 (1999) 781–786.
[27] R. Terzian, N. Serpone, Heterogeneous photocatalyzed oxidation of creosote components: mineralization of xylenols by illuminated TiO_2 in oxygenated aqueous media, J. Photochem. Photobiol. A: Chem. 89 (1995) 163–175.
[28] N. Daneshvar, M. Rabbani, N. Modirshahla, M.A. Behnajady, Kinetic modeling of photocatalytic degradation of acid red 27 in UV/TiO_2 process, J. Photochem. Photobiol. A: Chem. 168 (2004) 39–45.
[29] A.A. Khodja, T. Sehili, J.F. Pilichowski, P. Boule, Photocatalytic degradation of 2-phenylphenol on TiO_2 and ZnO in aqueous suspensions, J. Photochem. Photobiol. A: Chem. 141 (2001) 231–239.
[30] J. March, Advanced Organic Chemistry: Reactions, Mechanisms and Structure, 3rd ed., John Wiley and Sons, 1985.
[31] D.L. Pavia, G.M. Lampman, D.L. Kriz, Introduction to Spectroscopy: A Guide for Students, 3rd ed., Saunders College Publishing, 2000.
[32] J. Saien, R.R. Ardjmand, H. Iloukhani, Photocatalytic decomposition of sodium dodecyl benzene sulfonate under aqueous media in the presence of TiO_2, Phys. Chem. Liq. 41 (2003) 519–531.
[33] K. Vasanth Kumar, K. Porkodi, A. Selvaganapathi, Constrain in solving Langmuir–Hinshelwood kinetic expression for the photocatalytic degradation of Auramine O aqueous solutions by ZnO catalyst, Dyes Pigments 75 (2007) 246–249.
[34] J. Saien, S. Khezrianjoo, Degradation of the fungicide carbendazim in aqueous solutions with UV/TiO_2 process: optimization, kinetics and toxicity studies, J. Hazard. Mater. 157 (2008) 269–276.